Available online at www.sciencedirect.com
ScienceDirect
Journal of Organometallic Chemistry 692 (2007) 20–25
Journal of Organometallic Chemistry
www.elsevier.com/locate/jorganchem

Synthesis and X-ray structures of heptanuclear and decanuclear mixed-metal sulfido clusters containing noble metals and Group 15 metals

Kazumasa Oya, Takahiko Amitsuka, Hidetake Seino, Yasushi Mizobe *

Institute of Industrial Science, The University of Tokyo, Komaba, Meguro-ku, Tokyo 153-8505, Japan

Received 1 March 2006; accepted 24 April 2006
Available online 3 September 2006

Abstract

Reactions of incomplete cubane-type clusters $[(Cp^{\circ}RuCl)_2(\mu\text{-}SH)(\mu\text{-}SM'Cl_2)]$ (M′ = Sb (**2a**), Bi; $Cp^{\circ} = \eta^5\text{-}C_5Me_4Et$) with 0.5 equiv of $[PdCl_2(cod)]$ (cod = 1,5-cyclooctadiene) afforded the corner-shared double cubane-type clusters $[\{(Cp^{\circ}Ru)(Cp^{\circ}RuCl)(\mu\text{-}SM'Cl_2)\}_2(\mu_3\text{-}S)_2(\mu\text{-}Cl)_2Pd]$ (**3a**: M′ = Sb, **3b**: M′ = Bi) in moderate yields, whereas treatment of **2a** with 0.75 equiv of $[PdCl_2(cod)]$ gave the corner-shared triple cubane-type cluster $[\{(Cp^{\circ}Ru)(Cp^{\circ}RuCl)(\mu\text{-}SSbCl_2)(\mu_3\text{-}S)_2(\mu\text{-}Cl)_2Pd\}_2(Cp^{\circ}Ru)_2]$ (**4**). Single-crystal X-ray analyses have disclosed the detailed structures of novel heptanuclear and decanuclear mixed-metal cores for **3a** and **4**, respectively.

Keywords: Heptanuclear cluster; Decanuclear cluster; Palladium-ruthenium-antimony sulfido cluster; Palladium-ruthenium-bismuth sulfido cluster; X-ray structure

1. Introduction

Previously we reported the syntheses of the cubane-type mixed-metal sulfido clusters $[(Cp'MCl)_2(\mu\text{-}SM'Cl_2)_2]$ (**1**) (M = Ru: Cp′ = Cp°; M = Ir, Rh: Cp′ = Cp*; M = Sb, Bi; $Cp^{\circ} = \eta^5\text{-}C_5Me_4Et$, $Cp^* = \eta^5\text{-}C_5Me_5$) from the reactions of the versatile precursors to the homo- and heterometallic sulfido clusters $[(Cp'MCl)_2(\mu\text{-}SH)_2]$ with $M'Cl_3$ [1]. Subsequent studies on these reactions disclosed further that by treatment with 1 equiv of $M'Cl_3$ the Ru complex $[(Cp^{\circ}RuCl)_2(\mu\text{-}SH)_2]$ was able to be converted into the well-defined monopnictogen clusters $[(Cp^{\circ}RuCl)_2(\mu\text{-}SH)(\mu\text{-}SM'Cl_2)]$ (**2a**: M′ = Sb, **2b**: M′ = Bi) [2]. These reactions affording **1** and **2** represent the rare examples of the methods to prepare mixed-metal sulfido clusters containing both transition metals and Group 15 metals in a rational manner. Transition metal-Group 15 metal clusters are of much interest because of their possible relevance to the active sites of certain industrial heterogeneous catalysts [3].

Since clusters **2** still contain the reactive μ-SH ligand, these are also expected to serve as good precursors to the trimetallic clusters, and indeed it has already been demonstrated that the reaction of **2a** with $[Pd(PPh_3)_4]$ gives $[(Cp^{\circ}Ru)(Cp^{\circ}RuCl)(\mu\text{-}SSbCl_2)\{PdCl(PPh_3)\}(\mu_3\text{-}S)(\mu\text{-}H)]$ via the oxidative addition of the Pd(0) center across the S–H bond in **2a** [2]. Now we have found that the reactions of **2** with the Pd(II) complex $[PdCl_2(cod)]$ (cod = 1,5-cyclooctadiene) result in the formation of novel heptanuclear and decanuclear Ru–Pd–M′ trimetallic clusters. In this paper we wish to describe the details of their synthesis and X-ray structures.

2. Results and discussion

Dropwise addition of the CH_2Cl_2 solution containing 0.5 equiv of $[PdCl_2(cod)]$ into the CH_2Cl_2 solution of **2a**

* Corresponding author. Tel.: +81 3 5452 6360; fax: +81 3 5452 6361.
E-mail address: ymizobe@iis.u-tokyo.ac.jp (Y. Mizobe).

0022-328X/$ - see front matter © 2006 Elsevier B.V. All rights reserved.
doi:10.1016/j.jorganchem.2006.04.050

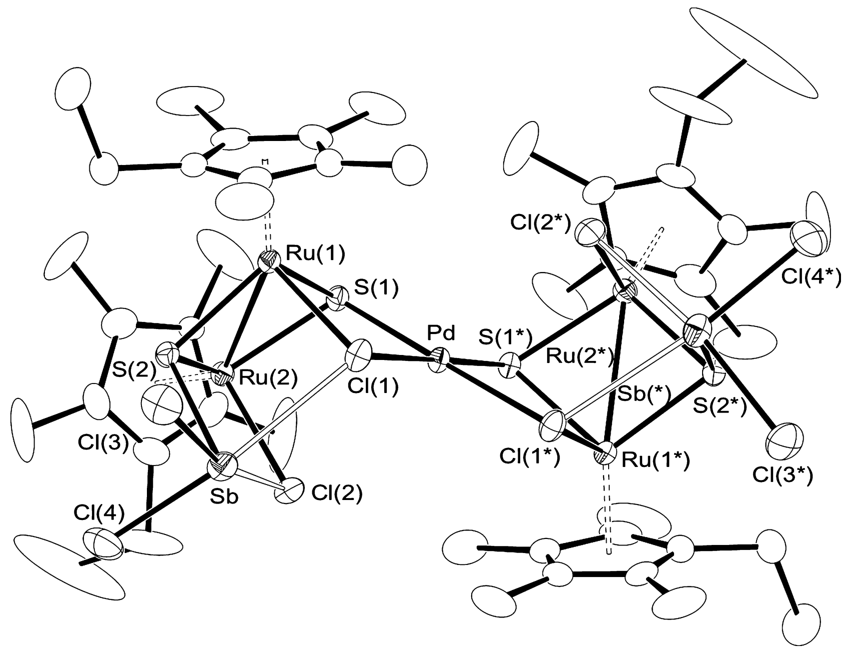

Fig. 1. An ORTEP drawing for **3a**. Thermal ellipsoids are drawn at the 30% probability level. One of the two disordered Cp° ligands on Ru(2) is shown. Solvating CH_2Cl_2 molecule as well as all hydrogen atoms are omitted for clarity.

or **2b** at 0 °C, followed by the continuous stirring of this mixture at room temperature, afforded the heptanuclear cluster $[\{(Cp^{\circ}Ru)(Cp^{\circ}RuCl)(\mu\text{-}SM'Cl_2)\}_2(\mu_3\text{-}S)_2(\mu\text{-}Cl)_2Pd]$ (**3a**: M′ = Sb, **3b**: M′ = Bi) in moderate yields (Eq. (1)). The X-ray analysis by the use of a single crystal of **3a** has disclosed the corner-shared double cubane-type structure for **3**, in which two incomplete cubane-type $Ru_2M'S_2Cl_2$ cores of **2** are connected by one Pd incorporated into their void vertices with concomitant dehydrochlorination. An ORTEP drawing for **3a** is shown in Fig. 1, while selected interatomic distances and angles therein are listed in Table 1.

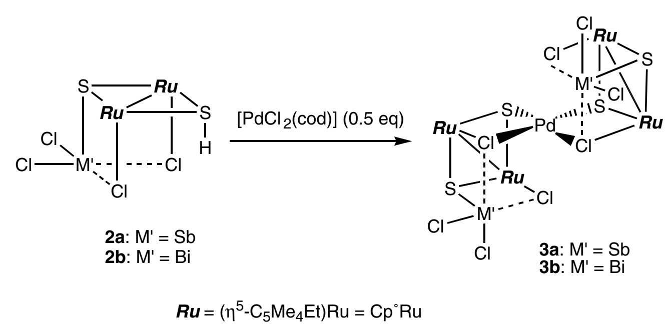

(1)

Table 1
Selected interatomic distances and angles in **3a**

(a) Distances (Å)			
Ru(1)–Ru(2)	2.8319(4)		
Pd–S(1)	2.246(1)	Pd–Cl(1)	2.477(1)
Ru(1)–S(1)	2.306(1)	Ru(1)–S(2)	2.319(1)
Ru(1)–Cl(1)	2.503(1)	Ru(2)–S(1)	2.298(1)
Ru(2)–S(2)	2.325(1)	Ru(2)–Cl(2)	2.445(1)
Sb–S(2)	2.486(1)	Sb–Cl(3)	2.449(2)
Sb–Cl(4)	2.429(2)	Sb—Cl(1)	2.952(1)
Sb—Cl(2)	2.792(1)		
Pd···Ru(1)	3.3841(3)	Pd···Ru(2)	3.7686(4)
(b) Angles (°)			
S(1)–Pd–S(1)*	90.56(4)	S(1)–Pd–Cl(1)	88.75(4)
Cl(1)–Pd–Cl(1)*	91.96(4)	S(1)–Ru(1)–S(2)	103.44(4)
S(1)–Ru(1)–Cl(1)	86.81(4)	S(2)–Ru(1)–Cl(1)	88.14(4)
S(1)–Ru(2)–S(2)	103.49(4)	S(1)–Ru(2)–Cl(2)	93.62(4)
S(2)–Ru(2)–Cl(2)	87.16(4)	S(2)–Sb–Cl(3)	87.64(5)
S(2)–Sb–Cl(4)	89.89(5)	Cl(3)–Sb–Cl(4)	93.65(6)

Cluster **3a** has a crystallographically imposed C_2 axis passing through the midpoints of Cl(1)–Cl(1)* and S(1)–S(1)* vectors as well as the Pd atom. The geometry around the Pd(II) center is square planar with two mutually cis μ_3-S lignads as well as two cis μ_2-Cl ligands. The separations of the Pd atom from the Ru atoms by 3.3841(3) and 3.7686(4) Å indicate the absence of any metal–metal bonding interactions between Pd and Ru. The Pd–μ_3-S bond distance at 2.246(1) Å is almost comparable to those in the Pd_2Ru_2 cluster $[(Cp^*Ru)_2(\mu_3\text{-}S)_2\{Pd(PPh_3)\}_2(\mu_2\text{-}Cl)]Cl$ [4] (2.226(2) and 2.229(2) Å), whereas the Pd–μ_2-Cl bond length at 2.477(1) Å is considerably longer than that at 2.409(2) Å in this Pd_2Ru_2 cluster, owing to the strong trans influence exerted by the S ligand in the former **3a**. For comparison, the lengths of mutually trans Pd–μ_3-S and Pd–$Cl_{terminal}$ bonds around square planar Pd atom in $[\{Cp^*Ru(CO)\}_2\{PdCl(PPh_3)\}_2(\mu_3\text{-}S)_2]$ are 2.241(2) and 2.378(2) Å [4] and those in $[(Cp^{\circ}Ru)(Cp^{\circ}RuCl)(\mu\text{-}SSbCl_2)\text{-}\{PdCl(PPh_3)\}(\mu_3\text{-}S)(\mu\text{-}H)]$ are 2.243(3) and 2.362(4) Å [2], respectively.

As for the incomplete cubane-type $Ru_2SbS_2Cl_2$ unit in **3a**, all metrical parameters are in good agreement with those in the parent cluster **2a** [2] except for those associated with Cl(1). Thus, the Cl(1) atom, which was bonded to Ru(1) at the bond length of 2.418(1) Å and weakly interacting with Sb by the separation of 2.811(1) Å in **2a**, is bridging between the Ru(1) and Pd atoms and weakly connected with the Sb atom in **3a**, where the Ru(1)–Cl(1) bond distance is elongated to 2.503(1) Å and the Sb–Cl(1) separation increases to 2.952(1) Å, respectively. The Ru–Ru distance at 2.8319(4) Å is typical as the Ru–Ru single bond distance bridged by two thiolato or hydrosulfido ligands [1,5], and the diamagnetic nature of **3** containing four Ru(III) centers is interpreted in terms of the spin pairing by the presence of two Ru–Ru single bonds.

Although two Cp° ligands in one incomplete cubane are not equivalent, the ^{1}H NMR spectra of both **3a** and **3b** dissolved in $CDCl_3$ and CD_2Cl_2 show only one set of signals due to the Cp° ligands, indicating the fluxional feature of **3** in solution. Upon decreasing the recording temperature to −70 °C, these signals broadened significantly but did not separate to two sets. Quite long Pd–Cl bond distances in **3a** demonstrated by the X-ray analysis suggest that dissociation of the Cl ligands from Pd may easily occur for **3** in solution, and subsequent rotation of the incomplete cubane-type cores around the Pd–S bonds prior to the coordination of the other Cl atoms to Pd presumably results in the equivalence of all Cp° ligands in the ^{1}H NMR time scale.

Interestingly, from the reaction of **2a** with 0.75 equiv of $[PdCl_2(cod)]$, a decanuclear cluster $[\{(Cp°Ru)(Cp°RuCl)(\mu\text{-}SM'Cl_2)(\mu_3\text{-}S)_2(\mu\text{-}Cl)_2Pd\}_2(Cp°Ru)_2]$ (**4**) was isolated in 20% yield (Eq. (2)) and its unique corner-shared triple cubane-type structure has been determined successfully by the X-ray analysis. Significant amount of **3a** was also present in the reaction mixture, which was confirmed by the ^{1}H NMR spectrum of the evaporated reaction mixture residue. The crystal of **4** contained two essentially identical but crystallographically independent chiral molecules. An ORTEP drawing of one molecule is shown in Fig. 2, while the selected metrical parameters in this molecule as well as those of the corresponding linkages in the other molecule are listed in Table 2.

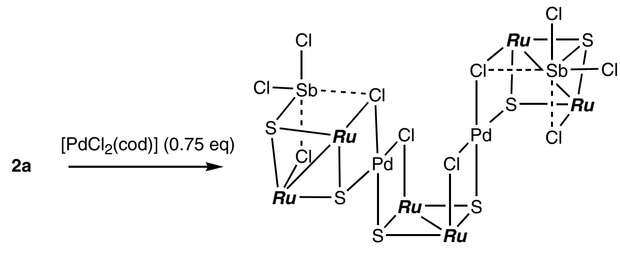

(2)

As shown in Fig. 2, **4** has a decanuclear core in which three cubane-type units are connected by two square planar Pd atoms in a corner-shared fashion. The structures of the two terminal cubanes in **4** are essentially the same as that in **3a** and corresponding interatomic distances and angles therein are in good agreement to each other. The central cubane consists of two three-legged piano stool Ru centers, two μ_3-sulfides, and two μ_2-chlorides in addition to two Pd atoms. The Ru–Cl bond lengths associated with the Cl ligands bridging between Ru and Pd in this core (2.484(8)–2.497(8) Å) are considerably longer than those of the μ_2-Cl ligands in the terminal cubanes bonded to Ru and weakly to Sb (2.442(9)–2.458(9) Å), but slightly shorter than those of the μ_3-Cl ligand bonded weakly to Sb in addition to Pd and Ru (2.507(8)–2.532(8) Å). As for the Pd–μ_2-Cl bond distances, those in the terminal cubanes with respect to the Cl ligands interacting further to the Sb atoms (2.483(8)–2.499(7) Å) are significantly longer than those associated with the central cubane (2.413(8)–2.439(7) Å).

Cluster **4** is presumed to be available from the reaction of 1 equiv of **2a**, 2 equiv of $[(Cp°RuCl)_2(\mu\text{-}SH)_2]$ generated in situ, and 2 equiv of $[PdCl_2(cod)]$ through dehydrochlorination. However, reactions of these three complexes in the ratios such as 2:1:2, 2:2:3, and 2:3:4 resulted in the isolation of **3a** as the sole characterizable product. Studies are still continuing to develop the rational methods to derivatize

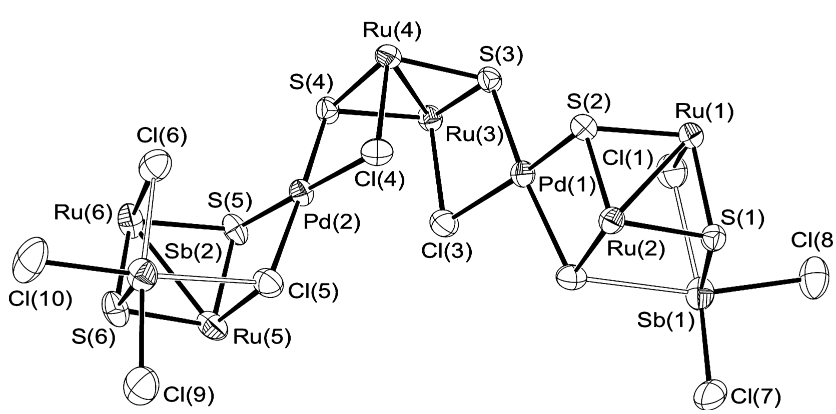

Fig. 2. An ORTEP drawing for one of the two independent molecules of **4**. Thermal ellipsoids are drawn at the 30% probability level. All Cp° ligands and solvating THF molecules are omitted for clarity.

Table 2
Selected interatomic distances and (Å) angles (°) in **4**

	Molecule			Molecule	
	1	2		1	2
(a) Distances					
Ru(1)–Ru(2)	2.836(3)	2.843(4)	Ru(3)–Ru(4)	2.810(3)	2.813(3)
Ru(5)–Ru(6)	2.834(4)	2.846(3)			
Pd(1)–S(2)	2.264(8)	2.212(8)	Pd(1)–S(3)	2.249(7)	2.246(8)
Pd(1)–Cl(2)	2.483(8)	2.493(8)	Pd(1)–Cl(3)	2.436(8)	2.417(8)
Pd(2)–S(4)	2.261(7)	2.270(7)	Pd(2)–S(5)	2.216(8)	2.244(7)
Pd(2)–Cl(4)	2.439(7)	2.413(8)	Pd(2)–Cl(5)	2.492(8)	2.499(7)
Ru(1)–S(1)	2.312(8)	2.302(8)	Ru(1)–S(2)	2.293(8)	2.289(7)
Ru(1)–Cl(1)	2.442(9)	2.454(8)	Ru(2)–S(1)	2.308(7)	2.301(8)
Ru(2)–S(2)	2.300(8)	2.295(8)	Ru(2)–Cl(2)	2.532(8)	2.515(8)
Ru(3)–S(3)	2.302(7)	2.291(8)	Ru(3)–S(4)	2.295(7)	2.289(7)
Ru(3)–Cl(3)	2.484(8)	2.497(8)	Ru(4)–S(3)	2.258(7)	2.280(7)
Ru(4)–S(4)	2.298(7)	2.326(7)	Ru(4)–Cl(4)	2.493(8)	2.488(7)
Ru(5)–S(5)	2.303(8)	2.299(7)	Ru(5)–S(6)	2.310(9)	2.319(8)
Ru(5)–Cl(5)	2.507(8)	2.532(8)	Ru(6)–S(5)	2.297(8)	2.284(7)
Ru(6)–S(6)	2.317(9)	2.328(8)	Ru(6)–Cl(6)	2.452(9)	2.458(9)
Sb(1)–S(1)	2.495(8)	2.474(8)	Sb(1)–Cl(7)	2.452(9)	2.47(1)
Sb(1)–Cl(8)	2.45(1)	2.39(1)	Sb(2)–S(6)	2.474(9)	2.512(8)
Sb(2)–Cl(9)	2.46(1)	2.46(1)	Sb(2)–Cl(10)	2.41(1)	2.38(1)
Sb(1)—Cl(1)	2.776(9)	2.793(8)	Sb(1)—Cl(2)	2.874(8)	2.993(8)
Sb(2)—Cl(5)	2.958(8)	2.960(8)	Sb(2)—Cl(6)	2.794(9)	2.764(9)
Pd(1)···Ru(1)	3.808(3)	3.796(3)	Pd(1)···Ru(2)	3.339(3)	3.314(3)
Pd(1)···Ru(3)	3.368(3)	3.349(3)	Pd(1)···Ru(4)	3.780(3)	3.797(3)
Pd(2)···Ru(3)	3.772(3)	3.803(3)	Pd(2)···Ru(4)	3.436(3)	3.412(3)
Pd(2)···Ru(5)	3.453(3)	3.383(3)	Pd(2)···Ru(6)	3.740(3)	3.779(3)
(b) Angles					
S(2)–Pd(1)–S(3)	90.5(3)	88.1(3)	S(2)–Pd(1)–Cl(2)	90.5(3)	90.3(3)
S(3)–Pd(1)–Cl(3)	89.1(3)	89.6(3)	Cl(2)–Pd(1)–Cl(3)	91.2(3)	92.8(3)
S(4)–Pd(2)–S(5)	91.6(3)	91.8(3)	S(4)–Pd(2)–Cl(4)	87.4(3)	88.7(3)
S(5)–Pd(2)–Cl(5)	86.7(3)	89.3(2)	Cl(4)–Pd(2)–Cl(5)	94.3(3)	91.6(2)
S(1)–Ru(1)–S(2)	102.9(3)	102.9(3)	S(1)–Ru(1)–Cl(1)	89.3(3)	87.3(3)
S(2)–Ru(1)–Cl(1)	91.7(3)	93.4(3)	S(1)–Ru(2)–S(2)	102.8(3)	102.8(3)
S(1)–Ru(2)–Cl(2)	87.2(3)	90.1(3)	S(2)–Ru(2)–Cl(2)	88.5(3)	87.9(3)
S(3)–Ru(3)–S(4)	102.7(3)	104.1(3)	S(3)–Ru(3)–Cl(3)	86.7(3)	86.6(3)
S(4)–Ru(3)–Cl(3)	92.0(3)	91.5(2)	S(3)–Ru(4)–S(4)	104.0(3)	103.2(3)
S(3)–Ru(4)–Cl(4)	93.1(3)	93.9(3)	S(4)–Ru(4)–Cl(4)	85.3(2)	85.7(2)
S(5)–Ru(5)–S(6)	103.1(3)	102.9(3)	S(5)–Ru(5)–Cl(5)	84.5(3)	87.3(2)
S(6)–Ru(5)–Cl(5)	89.5(3)	90.1(3)	S(5)–Ru(6)–S(6)	103.1(3)	103.1(3)
S(5)–Ru(6)–Cl(6)	94.6(3)	93.9(3)	S(6)–Ru(6)–Cl(6)	86.2(3)	86.4(3)
S(1)–Sb(1)–Cl(7)	90.4(3)	83.9(3)	S(1)–Sb(1)–Cl(8)	88.5(3)	90.9(3)
Cl(7)–Sb(1)–Cl(8)	96.6(3)	93.0(4)	S(6)–Sb(2)–Cl(9)	88.2(3)	85.7(3)
S(6)–Sb(2)–Cl(10)	89.4(3)	92.0(3)	Cl(9)–Sb(2)–Cl(10)	93.9(4)	91.4(4)

the cluster oligomers and polymers in high yields through condensation between discrete cluster molecules.

3. Experimental

3.1. General consideration

All manipulations were carried out under N_2 using Schlenk techniques. Solvents were dried by common methods and distilled under N_2 before use. Complexes **2** were prepared as described previously [2], while [$PdCl_2$(cod)] was obtained according to the literature methods [6]. NMR spectra were measured on a JEOL alpha-400 spectrometer and elemental analyses were done with a Perkin–Elmer 2400 series II CHN analyzer.

3.2. Preparation of 3a

Into a stirred CH_2Cl_2 solution (5 cm^3) of **2a** (202 mg, 0.244 mmol) was added dropwise a CH_2Cl_2 solution (20 cm^3) of [$PdCl_2$(cod)] (34 mg, 0.12 mmol) at 0 °C. The mixture was gradually warmed to room temperature and continuously stirred for 12 h. The resultant green solution was dried up in vacuo and the residue was washed with 5 cm^3 of ether three times prior to the extraction with CH_2Cl_2 (20 cm^3). Addition of hexane (30 cm^3) to the concentrated extract (ca. 10 cm^3) gave **3a** as green crystals (152 mg, 72% yield). Although the single crystal for the X-ray analysis consisted of one solvating CH_2Cl_2 molecule per one **3a** molecule, crystals finally obtained after thorough drying contained only negligible amount of CH_2Cl_2

as confirmed by the ^{1}H NMR spectrum recorded in $CDCl_3$. Anal. Calc. for $C_{44}H_{68}Cl_8PdRu_4S_4Sb_2$: C, 29.97; H, 3.89. Found: C, 29.95; H, 3.68%. ^{1}H NMR ($CDCl_3$, ppm): 1.10 (t, $J = 7.6$ Hz, 12H, CH_2CH_3), 1.69 (s, 12H, CCH_3), 1.72 (s, 24H, CCH_3), 1.73 (s, 12H, CCH_3), 2.10–2.20 (m, 8H, CH_2CH_3).

3.3. Preparation of **3b**

This cluster was prepared similarly from **2b** (185 mg, 0.202 mmol) and [$PdCl_2$(cod)] (29 mg, 0.10 mmol). The yield was 143 mg (73%) as green crystals. Anal. Calc. for $C_{44}H_{68}Cl_8Bi_2PdRu_4S_4$: C, 27.28; H, 3.54. Found: C, 27.29; H, 3.25%. ^{1}H NMR ($CDCl_3$, ppm): 1.12 (t, $J = 7.6$ Hz, 12H, CH_2CH_3), 1.67, 1.70, 1.71, 1.73 (s, 12H each, CCH_3), 2.10–2.20 (m, 8H, CH_2CH_3).

3.4. Preparation of **4**

Cluster **2a** (17 mg, 0.020 mmol) and [$PdCl_2$(cod)] (4.2 mg, 0.015 mmol) was dissolved in THF (5 cm^3) and the mixture was stirred at room temperature. The color changed immediately to green and then to dark red over 12 h. The resultant mixture was dried up in vacuo, and the residue was washed three times with 3 cm^3 of ether and then extracted with THF (5 cm^3). Addition of hexane (10 cm^3) to the concentrated extract (3 cm^3) afforded **4** · 1.3THF (3.5 mg, 20% yield based on Ru). Anal. Calc. for $C_{71.2}H_{112.4}O_{1.3}Cl_{10}Pd_2Ru_6S_6Sb_2$: C, 32.90; H, 4.36. Found: C, 33.54; H, 4.34%. ^{1}H NMR ($CDCl_3$, ppm): 1.06 (t, $J = 7.6$ Hz, 6H, CH_2CH_3), 1.11 (t, $J = 7.6$ Hz, 12H, CH_2CH_3), 1.69, 1.70, 1.71, 1.73 (s, 12H each, CCH_3), 1.72 (s, 24H, CCH_3), 2.0–2.2 (m, 12H, CH_2CH_3).

Table 3
Details of X-ray crystallography for **3a** and **4**

	3a · CH_2Cl_2	**4** · 1.3THF
Formula	$C_{45}H_{70}Cl_{10}$-$PdS_4Ru_4Sb_2$	$C_{71.2}H_{112.4}Cl_{10}O_{1.3}$-$Pd_2S_6Ru_6Sb_2$
Formula weight	1848.00	2598.88
Space group	$C2/c$ (no. 15)	$P2_12_12_1$ (no. 19)
Unit cell dimensions		
a (Å)	14.119(3)	17.722(2)
b (Å)	16.683(3)	28.665(4)
c (Å)	26.149(4)	38.816(5)
β (°)	91.227(3)	90
V (Å^3)	6158(2)	19719(5)
Z	4	8
ρ_{calc} (g cm^{-3})	1.993	1.751
μ_{calc} (cm^{-1})	27.03	22.19
Crystal size (mm^3)	0.25 × 0.25 × 0.20	0.50 × 0.40 × 0.03
Number of unique data	7056	24654
Number of observed data	5083 ($I > 2\sigma(I)$)	12872 ($I > 3\sigma(I)$)
Transmission factor	0.422–0.582	0.592–0.936
R_1[a]	0.032	0.061
wR_2[b] or Rw[c]	0.104	0.072
Goodness-of-fit[d]	1.001	1.009
Residual peaks (e$^-$ Å^{-3})	1.57, −1.68	1.10, −1.15

[a] $R_1 = \sum||F_o| - |F_c||/\sum|F_o|$ (observed data).
[b] $wR_2 = [\sum(w(F_o^2 - F_c^2)^2)/\sum w(F_o^2)^2]^{1/2}$ (all data).
[c] $Rw = [\sum(w(F_o^2 - F_c^2)^2)/\sum w(F_o^2)^2]^{1/2}$ (observed data).
[d] Goodness-of-fit $= [\sum w(|F_o| - |F_c|)^2/\{(\text{no. observed}) - (\text{no. variables})\}]^{1/2}$.

3.5. X-ray crystallography

Single crystals of **3a** · CH_2Cl_2 and **4** · 1.3THF were sealed in glass capillaries under argon and mounted on a Rigaku Mercury-CCD diffractometer equipped with a graphite-monochromatized Mo Kα source. All diffraction studies were done at 23 °C, whose details are listed in Table 3.

Structure solution and refinements were carried out by using the CrystalStructure program package [7]. The positions of the non-hydrogen atoms were determined by Patterson methods (PATTY [8]) and subsequent Fourier synthesis (DIRDIF 99 [9]). In **3a**, the Cp° ligand bound to Ru(2) is disordered in two orientations with the occupancies of 0.55 and 0.45. Non-hydrogen atoms were refined anisotropically by minimizing wR_2 using all data, where full-matrix least-squares techniques are employed. For **4**, asymmetric unit in the crystal contained two independent molecules of **4**. The ethyl groups in three Cp° ligands are disordered in orientations, for which the ratios of occupancies are 0.5:0.5, 0.6:0.4, and 0.6:0.4. Solvating THF molecules were found at four positions with the occupancies of 1, 0.55, 0.45, and 0.6, respectively, among which the first one orients in two different directions in a ratio of 1:1. Refinements were done by minimizing $R1$ for the reflections $I > 3\sigma(I)$, where anisotropic parameters were applied to the Cl, Pd, S, Ru, and Sb atoms, whereas the O and C atoms were refined isotropically. The solvating THF molecules were refined with restraints. All hydrogen atoms in **3a** and **4** except for those attached to the disordered C atoms and in the THF molecules were placed at the calculated positions and included at the final stages of the refinements with fixed parameters. Absolute structure of **4** was determined by refinement of Flack parameter (−0.03(5)).

3.6. Supplementary material

Details of the X-ray analysis data for **3a** · CH_2Cl_2 and **4** · 1.3THF have been deposited with the Cambridge Crystallogaphic Data Centre, CCDC Nos. 299890 and 299891, respectively. Copies of this information may be obtained free of charge from The Director, CCDC, 12 Union Road, Cambridge CB2 1EZ, UK (fax: +44 1223 336033; e-mail: deposit@ccdc.cam.ac.uk or http://www.ccdc.cam.ac.uk).

Acknowledgements

This work was supported by Grant-in-Aid for Scientific Research on Priority Areas (No. 14078206, "Reaction Control of Dynamic Complexes") from the Ministry of Education, Culture, Sports, Science and Technology, Japan and by CREST of JST (Japan Science and Technology Agency).

References

[1] W.-Y. Yeh, H. Seino, T. Amitsuka, S. Ohba, M. Hidai, Y. Mizobe, J. Organomet. Chem. 689 (2004) 2338.

[2] T. Amitsuka, H. Seino, M. Hidai, Y. Mizobe, Organometallics 25 (2006) 3034.

[3] (a) Clusters containing transition metals and heavier Group 15 elements: see for example K.H. Whitmire, Adv. Organomet. Chem. 42 (1998) 1;
(b) J. Wachter, Angew. Chem., Int. Ed. 37 (1998) 750;
(c) O.J. Sherer, Angew. Chem., Int. Ed. Engl. 29 (1990) 1104;
(d) N.A. Compton, R.J. Errington, N.C. Norman, Adv. Organomet. Chem. 31 (1990) 91;
(e) H.J. Breunig, I. Ghesner, Adv. Organomet. Chem. 49 (2003) 95.

[4] S. Kuwata, K. Hashizume, Y. Mizobe, M. Hidai, Organometallics 21 (2002) 5401.

[5] (a) H. Matsuzaka, J.-P. Qü, T. Ogino, M. Nishio, Y. Nishibayashi, Y. Ishii, S. Uemura, M. Hidai, J. Chem. Soc., Dalton Trans. (1996) 4307;
(b) K. Hashizume, Y. Mizobe, M. hidai, Organometallics 15 (1996) 3303.

[6] D. Drew, J.R. Doyle, Inorg. Synth. 13 (1972) 52.

[7] D.J. Watkin, C.K. Prout, J.R. Carruthers, P.W. Betteridge, CRYSTALS Issue 10, CrystalStructure 3.6.0: Crystal Structure Analysis Package, Rigaku and Rigaku/MSC, 2000–2004, 9009 New Trails Dr., The Woodlands, TX 77381, USA.

[8] P.T. Beurskens, G. Admiraal, G. Beurskens, W.P. Bosman, S. Garcia-Granda, R.O. Gould, J.M.M. Smits, C. Smykall, PATTY, The DIRDIF program system, Technical Report of the Crystallography Laboratory: University of Nijmegen, Nijmegen, The Netherlands, 1992.

[9] P.T. Beurskens, G. Admiraal, G. Beurskens, W.P. Bosman, R. de Gelder, R. Israel, J.M.M. Smits, DIRDIF 99, The DIRDIF 99 Program System, Technical Report of the Crystallography Laboratory: University of Nijmegen, Nijmegen, The Netherlands, 1999.